Enhanced performance of InGaN/GaN multiple quantum well solar cells with double indium content*

Zhao Bi-Jun(赵璧君), Chen Xin(陈 鑫), Ren Zhi-Wei(任志伟),
Tong Jin-Hui(童金辉), Wang Xing-Fu(王幸福), Li Dan-Wei(李丹伟),
Zhuo Xiang-Jing(卓祥景), Zhang Jun(章 俊), and Yi Han-Xiang(易翰翔), and Li Shu-Ti(李述体)†,

Laboratory of Nanophotonic Functional Materials and Devices, Institute of Opto-Electronic Materials and Technology, South China Normal University, Guangzhou 510631, *China*

(Received 18 December 2012; revised manuscript received 18 January 2013)

The performance of a multiple quantum well (MQW) InGaN solar cell with double indium content is investigated. It is found that the adoption of a double indium structure can effectively broaden the spectral response of the external quantum efficiencies and optimize the overall performance of the solar cell. Under AM1.5G illumination, the short-circuit current density (J_{sc}) and conversion efficiency of the solar cell are enhanced by 65% and 13% compared with those of a normal single-indium-content MQW solar cell. These improvements are mainly attributed to the expansion of the absorption spectrum and better extraction efficiency of the photon-generated carriers induced by higher polarization.

Keywords: metal–organic chemical vapor deposition, GaN-based solar cells, InGaN/GaN multiple quantum wells

PACS: 84.60.Jt, 85.35.Be, 85.30.De **DOI:** 10.1088/1674-1056/22/8/088401

1. Introduction

Nowadays, indium gallium nitride ($In_xGa_{1-x}N$) alloys have attracted a lot of attention for optoelectronic applications[1–3] due to their tunable energy band gap varying from 0.7 eV to 3.4 eV.[4–9] The absorption range covers a major portion of the solar spectrum, making $In_xGa_{1-x}N$ a promising candidate for multi-junction solar cell systems. In addition, with high radiation resistance, thermal stability and chemical tolerance, InGaN solar cells could operate under extreme environments.[10]

However, a relatively high indium content ($x > 0.40$) is required in $In_xGa_{1-x}N$ to achieve a better spectral overlap in the solar spectrum and a higher conversion efficiency.[11,12] This is a challenge to epitaxial layer growth because of the large lattice mismatch between InN and GaN at high indium content. The critical layer thickness of the high indium content $In_xGa_{1-x}N$ layer is only about a few nanometers.[13] When the thickness and/or indium content in an InGaN alloy increases, it results in In-rich clusters and phase separation in the $In_xGa_{1-x}N$ layer. As a consequence, the performance of high indium content solar cells is lower than the theoretical prediction. To partially solve the problem, an $In_xGa_{1-x}N$ multiple quantum well (MQW) structure with a thin quantum well layer (< 5 nm) was introduced, which can keep the quantum well below the critical thickness and generate better crystalline quality. Recently, some reports have concentrated on the structure of the MQW,[14–19] however, their performance still has much room for improvement. One aspect is that single-In-content solar cells are limited to a narrow absorption spectrum, which leads to relatively low efficiency. In this paper, we introduce a double-In-content structure with two diverse indium content layers ($x_1 = 0.15$ and $x_2 = 0.23$). The high-energy photons can be captured by the upper layers (low In content), while low-energy photons can be absorbed by the under layers (high In content). The design of this structure has expanded the absorption spectrum and increased the absorption of low-energy photons, which results in the augmentation of J_{sc} and an improvement in overall efficiency.

2. Experiment

The solar cells were produced by metal–organic chemical vapor deposition (MOCVD) on (0001) sapphire substrates. Trimethylgallium (TMGa), trimethylindium (TMIn), and ammonia (NH_3) were used as the Ga, In, and N sources, respectively. SiH_4 and bis-cyclopentadienyl magnesium were injected into the reactor for n-type and p-type doping.

Figures 1(a) and 1(b) show the cross-sectional schematics of the epitaxial structures of the device with double In content and single In content, respectively.

The structure of sample A consists of a 1-μm thick unintentionally doped (UID) GaN buffer layer, a 2-μm Si-doped n-GaN layer ([Si] = 5×10^{18} cm^{-3}), an eight-period undoped

*Project supported by the National Natural Science Foundation of China (Grant No. 51172079), the Science and Technology Program of Guangdong Province, China (Grant Nos. 2010B090400456 and 2010A081002002), and the Science and Technology Program of Guangzhou City, China (Grant No. 2011J4300018).

†Corresponding author. E-mail: lishuti@scnu.edu.cn

© 2013 Chinese Physical Society and IOP Publishing Ltd

$In_{0.23}Ga_{0.77}N$(3 nm)/GaN(6 nm) multiple quantum well followed by an eight-period $In_{0.15}Ga_{0.85}N$(3 nm)/GaN(6 nm) multiple quantum well active region, and a 150-nm p-GaN top layer ([Mg] = 3×10^{17} cm^{-3}). After growing sample A, sample B was grown with the same structure except for the multiple quantum well active region, which comprised a 16-period undoped $In_{0.19}Ga_{0.81}N$(3 nm)/GaN(6 nm) multiple quantum well. The In content in the quantum wells of sample B stayed at 19%, remaining the same as the average In content in the quantum wells of sample A.

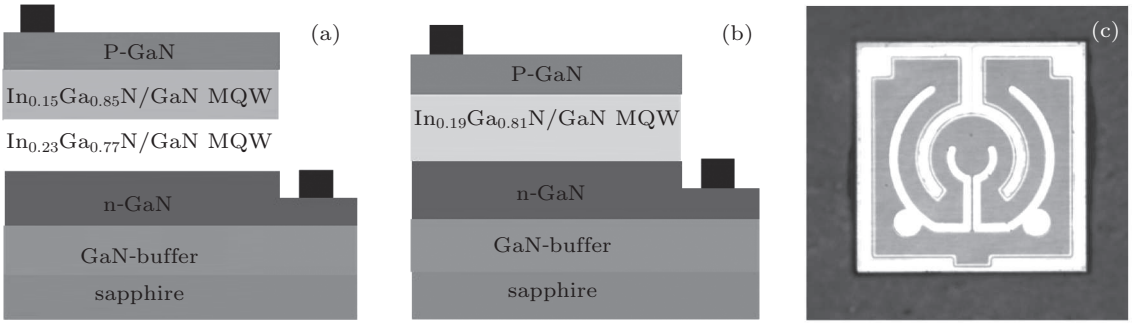


Fig. 1. Cross-sectional schematics of the epitaxial structures of (a) sample A with double In content, (b) sample B with single In content, and (c) patterns of solar cells with grid contact.

Following the MOCVD growth, the samples were characterized for crystalline perfection by X-ray diffraction (XRD) using an X'Pert materials research diffractometer (Philips). Then, photoluminescence (PL) measurements were performed using a 325 nm laser diode as the excitation source. In order to study the effects of the polarization fields in both samples, simulations were done using the APSYS software. As the parameters used to calculate the piezoelectric effect on InGaN vary, as shown in the literature, the simulation can give an indication of the general trend.

Samples were processed into solar cells each with 1 mm×1 mm size. The Ohmic contacts were formed with Ni/Au for the p-type and Ti/Al/Au for the n-type by annealing. Neither the current spreading layer nor the antireflection layer was used in the device. The patterns for solar cells with grid contact are shown in Fig. 1(c). Following the electrode fabrication, the performances of the solar cell were tested by external quantum efficiency (EQE) and illuminated current density versus voltage measurements (J–V). The EQE measurements were collected under monochromatic illumination using a xenon lamp in conjunction with a monochromator, and calibrated with a reference Si photodetector.

3. Results and discussion

The X-ray diffraction ω–2θ-scan spectra of samples A and B along the (002) direction are presented in Fig. 2. Three InGaN MQW satellite peaks can be observed in both samples. Through Philips X'pert simulation software, the In content values in the MQWs of samples A and B are calculated to be 15% and 23% (sample A with double In content) and 19% (sample B with double In content). The simulation results were all in accordance with our designed values. The full width at half maximum (FWHM) values for the (002) GaN of samples A and B are 292.7 arcsec and 296.2 arcsec, respectively. This fact indicates that the crystalline qualities are comparable to both samples,[20] which means that the double-In-content structure does not lead to inferior crystalline qualities compared with the common structure.[20]

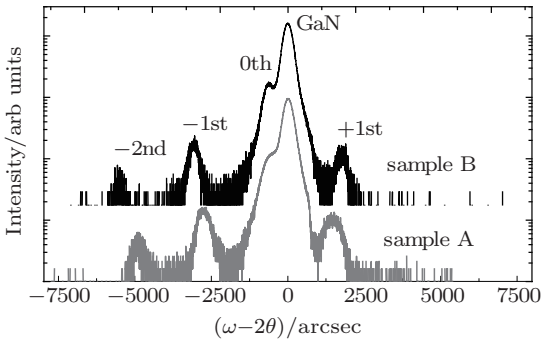


Fig. 2. X-ray diffraction ω–2θ-scan (002) spectra of samples A and B.

Figure 3(a) shows the room-temperature PL spectra of samples A and B. The MQW emission peak of sample B is centred at 467 nm, which corresponds to $In_{0.19}Ga_{0.81}N$. In sample B, the band-edge emission peaks of GaN that can be observed at 365 nm and 550 nm are the yellow band emission of GaN. Two MQW emission peaks can be observed in sample A. The first peak of sample A centred at 435 nm corresponds to $In_{0.15}Ga_{0.85}N$, and the second emission peak at 485 nm corresponds to $In_{0.23}Ga_{0.77}N$ and is relatively weak. One reason for the weak emission in the $In_{0.23}Ga_{0.77}N$ layer might be that the majority of photons are captured in the upper layer (In content 0.15) and join the photoluminescence process, which leads to less photons reaching the under layer (In content 0.23).

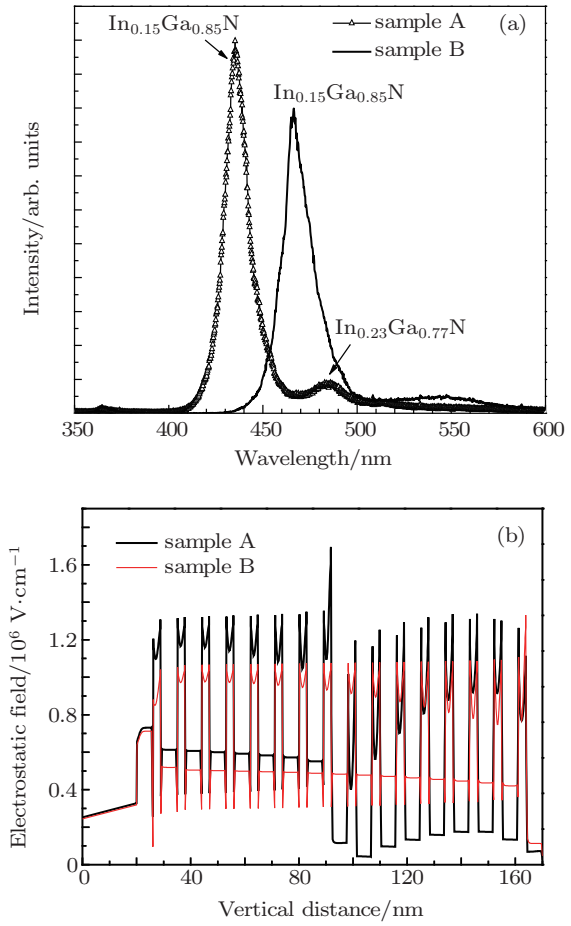


Fig. 3. (color online) (a) The PL emission spectra of samples A and B, and (b) the calculated results of the polarization fields in the MQW areas of samples A and B.

To further analyze this phenomenon, the configurations of samples A and B are modeled using the APSYS software.[21] The polarization fields in the MQW areas are shown in Fig. 3(b). It shows that the polarization fields in MQWs with higher In content ($x = 0.23$) are larger than those with lower In content. This may lead to a strong tilt in the energy band in quantum wells with higher In content, resulting in the separation of carriers and lower recombination rates in the photoluminescence process, which can explain the weaker photon emission in the under layer.

Figure 4 shows the the external quantum efficiency (EQE) versus excitation wavelength for samples A and B. The performances at short wavelengths (300 nm–360 nm) are almost the same for both samples, and the $\lambda < 360$ nm region is due to the light absorption of the GaN ($E_g = 3.4$ eV, $\lambda = 360$ nm) barrier layers. This can be seen in Fig. 4, where the absorption range of the MQW in sample B is from 360 nm to 430 nm, while sample A exhibits a broader spectral response, extending to 475 nm. Clearly, the results demonstrate that the adoption of a double indium structure can effectively broaden the spectral response of the external quantum efficiency. The reason for the enhancement of EQE at a longer wavelength is that more incident light at a longer wavelength can be absorbed by the modified structure.

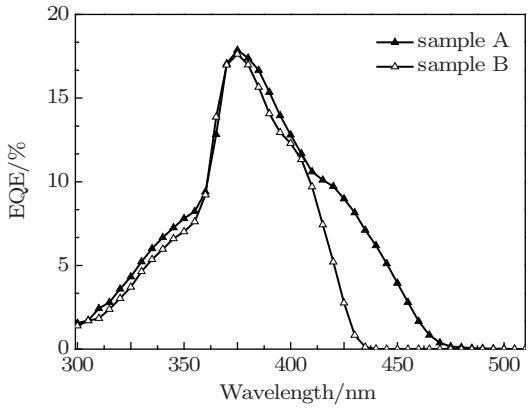


Fig. 4. Plots of external quantum efficiency, EQE, versus excitation wavelength for samples A and B.

Figure 5 shows the J–V characteristics of two fabricated $In_xGa_{1-x}N$/GaN MQW solar cells. The photovoltaic characteristics are summarized in Table 1. The values of V_{oc} are similar, varying only from 1.97 V to 2.01 V. The output voltage of the MQW solar cell is determined primarily by In content,[22] wider bandgap barrier material, recombination in the wells and in the barrier-well interfaces.[23] Nonradiative recombination processes significantly affect the output voltage behavior, and thus V_{oc} depends strongly on material quality. The average In content values of the two samples are both 0.19 and the barrier materials are the same. Moreover, the crystalline qualities are comparable for both samples. The factors discussed above lead to a comparable V_{oc}.

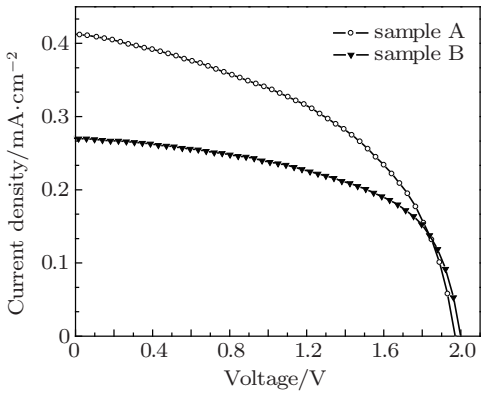


Fig. 5. The J–V curves for samples A and B under 1 sun AM 1.5 illumination.

Table 1. Summary of the device performance metrics for samples A and B.

Sample	V_{oc}/V	J_{sc}/(mA/cm^2)	FF/%	Conversion efficiency/%	P_{max}/(mW/cm^2)
A	1.97	0.41	48.80	0.34	0.39
B	2.01	0.27	56.04	0.30	0.30

The adoption of a double-In-content structure increases the short-circuit current density (J_{sc}) from 0.27 mA/cm^2 to 0.41 mA/cm^2 (65% increase). The improvement in J_{sc} can be attributed to two aspects. It is consistent with the trends observed in the EQE spectra where the double-In-content structure leads to expansion of the absorption solar spectrum, which means that more incident light of wavelengths in a wider range can be absorbed in the active region. Further, the higher polarization-induced fields in the modified structure prompt the separation of the photogenerated carrier and tunneling through the thin barriers, which also contributes to the improvement in J_{sc}.[24] The TD density of InGaN material grown on sapphire could be as high as 1×10^{10} cm^{-2},[24] thereby providing leakage paths and restraining the carrier transport. However, the high polarization fields could prompt the separation of the carriers before their recombination with each other or/and through these defect states. The barrier thickness of the structure is only 6 nm, which is thin enough for carrier tunneling. As shown in Fig. 2(b), the polarization fields in the under MQW layers of sample A are higher than the average value of sample B, which would be beneficial to the collection of the carriers. Although in the upper MQW layers, the polarization fields are slightly lower than those in the same areas of sample B, the overall polarization fields in sample A will be larger than those in sample B, which can lead to better extraction efficiency of the carrier in sample A.

4. Conclusions

In this paper, we demonstrate a double In content InGaN-based MQW solar cell with two different In content values. Under the illumination of 1.5G air mass, the proposed device achieves a fill factor of 48.80%, a short-circuit current density of 0.41 mA/cm^2, and an open circuit voltage of 1.97 V. The improvements in overall efficiency and J_{sc} are mainly due to the expansion of the absorbing spectrum and better transportation of photon-generated carriers.

References

[1] Muth J, Lee J, Shmagin I, Kolbas R, Casey J H, Keller B, Mishra U and DenBaars S 1997 *Appl. Phys. Lett.* **71** 2572

[2] Singh R, Doppalapudi D, Moustakas T and Romano L 1997 *Appl. Phys. Lett.* **70** 1089

[3] David A and Grundmann M 2010 *Appl. Phys. Lett.* **97** 033501

[4] Tong J T, Li S T, Liu T P, Liu C, Wang H L, Wu L J, Zhao B J, Wang X F and Chen X 2012 *Chin. Phys. B* **21** 118502

[5] Lu T P, Li S T, Zhang K, Liu C, Xiao G W, Zhou Y G, Zheng S W, Yin Y A, Wu L J, Wang H L and Yang X D 2011 *Chin. Phys. B* **20** 098503

[6] Wu L J, Li S T, Liu C, Wang H L, Lu T P, Zhang K, Xiao G W, Zhou Y G, Zheng S W, Yin Y A and Yang X D 2012 *Chin. Phys. B* **21** 068506

[7] Davydov V Y, Klochikhin A A, Seisyan R P, Emtsev V V, Ivanov S V, Bechstedt F, Furthmuller J, Harima H, Mudryi V, Aderhold J, Semchinova O and Graul J 2002 *Phys. Status Solidi B* 229 R1

[8] Wu J, Walukiewicz W, Yu K M, Shan W, Ager J W, Haller E E, Lu H, Schaff W J, Metzger W K and Kurtz S 2003 *J. Appl. Phys.* **94** 6477

[9] Xiao H L, Wang X L, Wang J X, Zhang N H, Liu H X, Zeng Y P, Li J M and Wang Z G 2005 *J. Crystals Growth* **276** 401

[10] Wu J, Walukiewicz W, Yu K M, Ager III J W, Haller E E, Lu H and Schaff W J 2002 *Appl. Phys. Lett.* **80** 4741

[11] Nanishi Y, Saito Y and Yamaguchi T 2003 *Jpn. J. Appl. Phys.* **42** 2549

[12] Wu J Q 2009 *Appl. Phys.* **106** 011101

[13] De Vos A 1992 *Endoreversible Thermodynamics of Solar Energy Conversion* (Oxford: Oxford University Press) p. 90

[14] Friedman D J 2010 *Curr. Solid State Mater. Sci.* **14** 131

[15] Holec D, Costa P M F J, Kappers M J and Humphreys C J 2007 *J. Crystals Growth* **303** 314

[16] Zhang X B, Wang X L, Xiao H L, Yang C B, Hou Q F, Yin H B, Chen H and Wang Z G 2011 *Chin. Phys. B* **20** 028402

[17] Dahal R, Pantha B, Li J, Lin J Y and Jiang H X 2009 *Appl. Phys. Lett.* **94** 063505

[18] Deng Q W, Wang X L, Xiao H L, Wang C M, Yin H B, Hong C, Hou Q F, Lin D F, Li J M, Wang Z G and Hou X 2011 *J. Phys. D: Appl. Phys.* **44** 265103

[19] Dahal R, Li J, Aryal K, Lin J Y and Jiang H X 2010 *Appl. Phys. Lett.* **97** 073115

[20] Sheu J K, Yang C C, Tu S T, Chang K H, Ming Lee L, Lai W C and Peng L C 2009 *IEEE Electron. Dev. Lett.* **30** 225

[21] Brown G F, Ager III J W, Walukiewicz W and Wu J 2010 *Sol. Energy Mater. Sol. Cells* **94** 478

[22] Chang J Y, Liou B T, Lin H W, Shih Y H, Chang S H and Kuo Y K 2011 *Opt. Lett.* **36** 3500

[23] Rimada J C, Hernandez L, Connolly J P and Barnham K W J 2007 *Microelectron. J.* **38** 513

[24] Yang C C, Sheu J K, Liang X W, Huang M S, Lee M L, Chang K H, Tu S J, Huang F W and Lai W C 2010 *Appl. Phys. Lett.* **97** 021113